New Diamond and Frontier Carbon Technology
Vol. 15, No. 5 2005
MYU Tokyo

NDFCT 492

Surface Transfer-Doping of H-Terminated Diamond with Adsorbates

Christoph E. Nebel*

Diamond Research Center, National Institute for Advanced Industrial Science and Technology, Tsukuba 305-8568, Japan

(Received 29 March 2005; accepted 27 May 2005)

Key Words: transfer doping, in-plane surface conductivity, surface electronic density of states

Hydrogen-terminated diamond films with Au and Al contacts have been investigated by contact potential difference measurements (CPD), *CV*-, *IV*- and Hall-effect experiments, and theoretical calculations in which the Schrödinger and Poisson equations have been solved to calculate the density-of-state (DOS) distribution at the surface of a hydrogen terminated diamond. From CPD experiments, we detect the Fermi energy of H-terminated diamond covered with an adsorbate layer in the valence band. The layer shows no contact potential difference to Au. For Al, a CPD of +588 V is detected, which indicates that the work function of Al is about 590 meV smaller than that of Au. Numerical calculations have been performed to elucidate the electronic band structure for hole sheet-carrier densities in the range of 10^{10} to 10^{13} cm^{-2}. These calculations reveal a 2D-DOS, with Fermi energies at about 240 to 880 meV below the valence-band maximum. The Schottky contact properties of Al are discussed on the basis of in-plane contact properties. Finally, temperature dependent variations of hole mobilities are discussed, revealing ion-induced scattering as the dominant scattering process at low temperatures; at higher temperatures, phonon scattering limits propagation. Based on the transfer doping model, the ionized impurities are located in the Helmholtz layer of the adsorbate film that covers the H-terminated diamond.

1. Introduction

Because of the outstanding electronic properties of diamond, it exhibits considerable potential for applications in electronic devices. In particular, two features of diamond are unique among all semiconductors: 1) the negative electron affinity (NEA) of hydrogen terminated diamond surfaces[1] and 2) the fairly high p-type surface conductivity, which can be detected under conditions that are closely related to the first feature. It appears that an adsorbate layer from the atmosphere on the hydrogen terminated diamond surface is required to induce a surface hole accumulation layer, as first reported by Landstrass and Ravi (1989).[2] Later, this observation was confirmed by several other groups, revealing the p-

*Corresponding author: e-mail: christoph.nebel@aist.go.jp

type nature of the conductive surface layer,[3,4] typical hole sheet densities between (10^{10}–10^{13}) cm^{-2},[4,5] and Hall mobilities between 1 and 100 cm^2/Vs.[5,6] The confusing mass of data about hole densities and mobilities resulting from the H-termination of diamond as published in the literature is summarized in Fig. 1.[7–14] Most researchers have applied different hydrogen termination parameters or even techniques (see Table 1),[10,15,16] with the result that a coherent picture is not obvious. There is an overall trend towards lower mobilities with increasing hole sheet densities, but the scatter in the data is large. In this paper we give some coherence to the experimental results primarily by examining Hall data detected in the temperature regime from 100 K to 500 K. The data under discussion have been detected on one sample by applying only one H-termination process but different thermal annealing and cleaning processes. We show that the mobilities of holes in the accumulation layer are governed by ionic scattering at low temperature and by phonon scattering at higher temperatures.

It is certain that the origin of the conductivity is related to hydrogen (for a review see refs. 1 and 17); however, several controversial models have been proposed as doping mechanisms, including (i) surface band bending due to hydrogen surface termination where valence-band electrons transfer into an adsorbate layer ("transfer doping model"),[18–20] (ii) shallow hydrogen induced acceptors,[3,21] and (iii) deep level passivation by hydrogen.[22] Our data, determined by temperature-dependent Hall-effect experiments, support clearly the transfer doping model.[16,23,24] In this model, valence band electrons tunnel into electronic empty states of an adjacent adsorbate layer, as shown schematically in Fig. 2. In order to act as a sink for electrons, the adsorbate layer must have its lowest unoccupied electronic level below the valence band maximum (VBM) of diamond. Maier *et al.*[20] proposed that for standard atmospheric conditions, the pH value of water is about 6 due to CO_2 content or other ionic contamination. They calculate the chemical potential μ_e for such an aqueous wetting layer to be about –4.26 eV. To calculate the valence band maximum E_{VBM} of H-terminated diamond with respect to the vacuum level E_{VAC} we take into account the band gap of

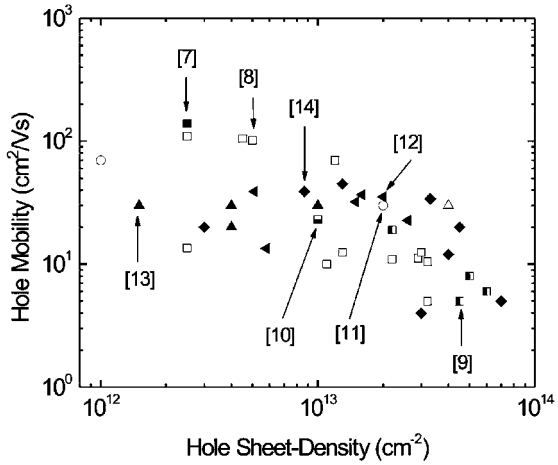

Fig. 1. Summary of hole mobilities and hole sheet densities as detected at room temperature on a variety of films. Data are from refs. 7–14.

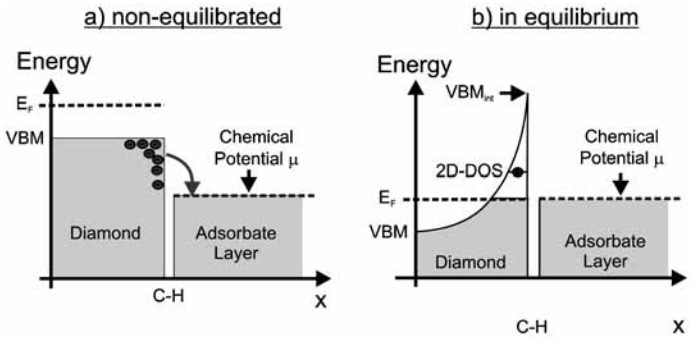

Fig. 2. Schematic drawing of the diamond/adsorbate heterojunction (a) for nonequilibrated and (b) equilibrated conditions. Electrons from the valence-band diffuse into empty electronic states of the adsorbate layer as long as the chemical potential μ_e is lower than the Fermi energy E_F.

diamond, E_G = 5.47 eV, and the negative electron affinity χ of –1.1 to –1.3 eV.[20,25] This results in an E_{VBM} of –4.17 to –4.37 eV if the vacuum level is zero. The pinning position of the Fermi-level E_F at the water/diamond interface is therefore in the range of about 90 meV in the valence band to 110 meV above E_{VBM}. A generalized summary of chemical potentials with respect to hydrogen- and oxygen-terminated diamond is given in Fig. 3.[26] It shows that for well-defined pH liquids with the chemical potential μ(pH) of adsorbate layers may indeed are below E_{VBM}. In such cases a hole accumulation layer at the surface of diamond is generated by transfer doping, as shown in Fig. 2. As the pH value of adsorbate layers cannot be detected experimentally, a discussion based on assumptions will not elucidate the real features. To characterize the surface properties of H-terminated diamond covered with an adsorbate layer, we have applied contact potential difference experiments ("Kelvin force.") The results are briefly introduced and discussed with respect to Schottky junction data detected on Al/diamond and Au/diamond combinations.

2. Experimental

To clean the surface of the diamond films, the samples were first boiled in aqua regia (a mixture of hydrochloric acid and nitric acid) to remove metals, followed by wet chemical etching in a CrO_3/H_2SO_4 solution at 180°C for one hour to removed graphitic parts from the surface and to oxidize the surfaces. After these procedures the samples were hydrogen terminated and characterized by wetting angle experiments and SEM. Hydrogenation was performed, using microwave plasma or hot filament techniques. The applied parameters are summarized in Table 1. It is interesting to note that all four applied processes resulted in sometimes high and sometimes low electronic properties. On the basis of our data it is therefore not possible to clearly identify the "best" way to achieve high sheet carrier densities and high mobilities. We leave this problem to further discussions and research activities.

The quality of the surface morphologies of our samples varied in the range between atomically flat (100)-oriented homoepitaxially grown diamond layers (CVD), natural type IIa diamonds with etching grooves in the range of several nanometers, and polycrystalline CVD diamond films with a roughness of up to several micrometers.

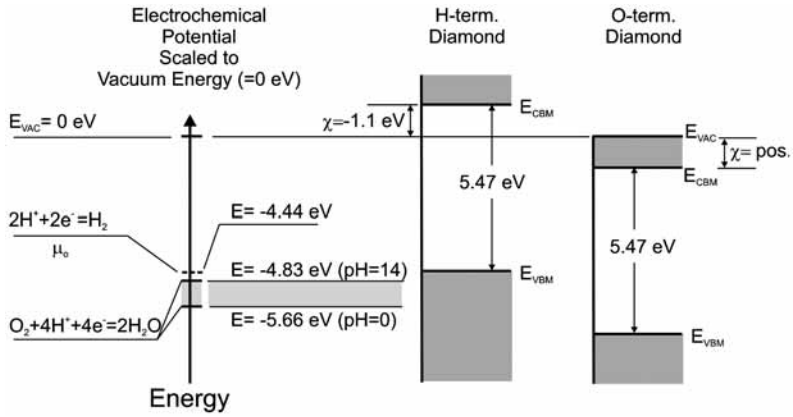

Fig. 3. Relationship between the chemical potential referred to the standard hydrogen electrode and the semiconductor energies referred to the vacuum level. The electron energies for the couple $O_2 + 4H^+ + 4e^- = H_2O$ at pH 0 and 14 are shown along with the band edges for hydrogen-terminated and oxidized diamond. The negative electron affinity was assumed to be –1.1 eV on H-terminated diamond.[26]

Table 1
Parameters for hydrogen termination of diamond.

Address	University College of London (UK)[10]	LIST (France)[16]	Diamond Center, AIST (Japan)[15]	Institute for Technical Physics, University Erlangen, Germany[16]
Technique	Microwave Plasma (2.45 GHz)	Microwave Plasma (2.45 GHz)	Microwave Plasma (2.45 GHz)	Hot Filament
Power (W)	800	900	750	2200°C Tungsten Temperature
Substrate Temperature (°C)	500	820	800	690
Pressure (Torr)	40	38	25	38
Duration (Minutes)	5	60	5	10
H_2-Flow (sccm)	100	120	400	100

Insolated hydrogen-terminated patterns on the diamond surface have been realized by oxygen plasma treatment through photolithographic masks. Ohmic contacts on hydrogen-terminated diamond have been generated by the thermal evaporation of Au (30–200 nm) in van de Pauw or Hall-bar configurations. To characterize aluminum as a Schottky junction on H-terminated diamond, areas of different sizes have been thermally evaporated. In this case, we used undoped, homoepitaxially grown (100) monocrystalline CVD diamond as a substrate.

The surface conductivity is generated by a “nondefined” adsorbate layer, which forms on the surface by exposure of the sample to air. All experimental results are therefore dependent on the history of the sample or on experimental details like vacuum conditions, thermal annealing, and pretreatments. To achieve reproducibility, the samples were

exposed to air for comparable periods of time. The Hall-effect experiments were carried out using identical parameters (vacuum and temperature variations), or in some cases special conditions were applied like fast cooling or thermal annealing. In the following, the results are discussed taking into account the specific parameters used.

3. Results

3.1 *Contact potential difference (CPD) experiments*

To collect experimental evidence for the transfer doping model, we carried out AFM and contact potential difference (CPD) experiments on atomically flat homo-epitaxially grown undoped CVD diamond. CPD measurements were performed to characterize the surface Fermi-energy with respect to Au and Al (for details see ref. 16). Au was used to calibrate the CPD experiments as Au is inert towards oxidation or other chemical reactions. The work-functions χ_{Au} of the gold contacts were measured by secondary photoelectron emission experiments and were found to be $\chi_{Au} = 4.3\ (\pm 0.1)$ eV.[25] This is slightly smaller than the values of 4.9 to 5.1 eV reported in the literature for polycrystalline Au.[27] A typical scanning electron microscopy image (SEM) and a related 2D CPD image as detected on a diamond sample that had been partially covered with Au (region A), partially hydrogenated (region B) and partially oxidized (region C) are shown in Figs. 4(a) and 4(b). In Fig. 4(c) a line scan in units of potential (mV) (white line in Fig. 4(b)) is shown; it reveals no difference between Au and H-terminated diamond. The oxidized areas appear dark in the SEM image, which is a result of the lower electron emissivity from these areas due to the positive electron affinity, whereas the hydrogen-terminated surface is bright due to its negative electron affinity. Figure 5 summarizes the result schematically, taking into account the negative electron affinity of –1.3 eV and the surface energies detected with respect to the work function χ_{Au} of Au.

CPD measurements on Al contacts on H-terminated diamond result in a surface potential difference of +588 mV. The work function of Al, $\chi_{Al} = 3.7$ eV, is smaller than the work function of Au. This is an effective work function of Al, as we assume that the surface of Al is partially oxidized. This result and the data for Au are shown in Fig. 5. The results indicate that the Fermi level of H-terminated diamond with an adsorbate layer is slightly in the valence band (in this case, about 130 meV). Such a shift of Fermi level is only possible if the Fermi level is not pinned by defects at the surface. Obviously, the optimized H termination generates such a defect free diamond surface and it is a perfect interface for liquids for electrochemical applications and for solids like metals or other candidates for heterojunction applications.

Taking into account these results, we expect ohmic properties for Au, as the Fermi level of Au is perfectly aligned with H-terminated diamond, whereas for Al the Fermi level is above the VBM, which gives rise to Schottky behavior. The surface energies of Au, Al and of H-terminated diamond covered with an adsorbate layer are shown in Fig. 6 and are discussed in the following.

3.2 *Current-voltage (IV) properties*

To characterize the properties of Al contacts, we have evaporated square Al contacts (600 nm thick) of different sizes surrounded by Au contacts separated by 400 μm using

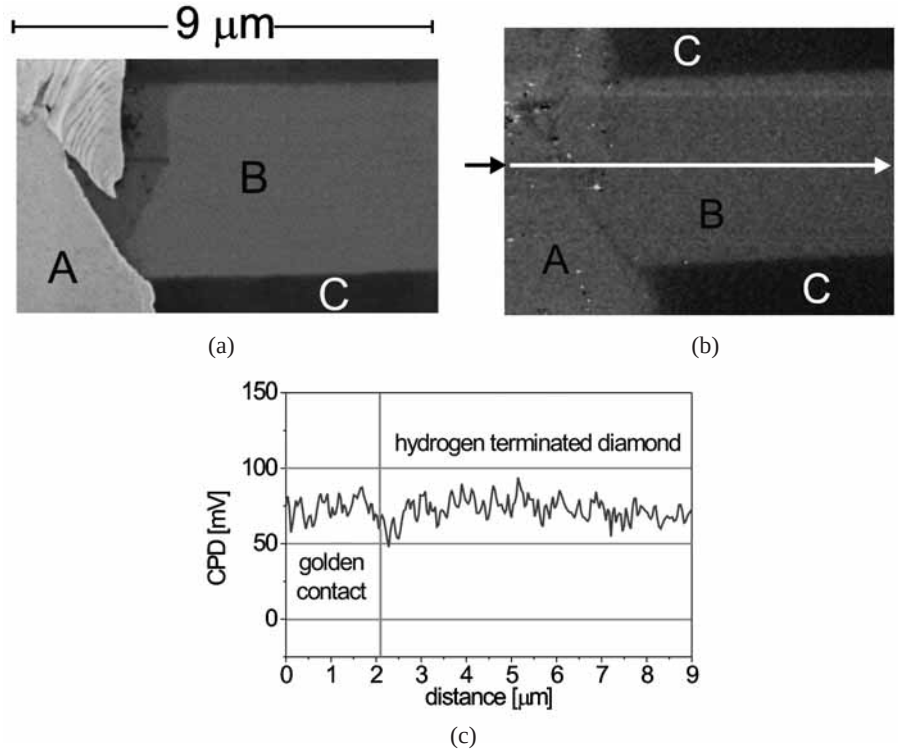

Fig. 4. (a) Scanning electron microscopy image of a diamond which has been partially covered with Au (A), hydrogen terminated (B) and oxidized (C). (b) Two-dimensional contact potential measurement (CPD) on a sample (see Fig. 4(a)). (c) The white line in Fig. 4(b) indicates the scan position of the spatial CPD profile shown here. Note: within experimental accuracy, no contact potential difference between Au and H-terminated diamond can be detected.

photolithographic masks. The thickness of the Au electrodes was 400 nm. The Au contacts show perfect ohmic characteristics. Three sizes of square Al electrodes were used: 50×50 μm^2, 100×100 μm^2, and 250×250 μm^2. Current-voltage measurements (*IV*) at 300 K in air on the 250 µm × 250 µm pats reveal Schottky characteristics due to Al, as shown in Fig. 7. Applying negative voltages of more than 0.6 V (threshold voltage) to the Al contacts gives rise to an exponential increase of the current over 7 orders of magnitude with an ideality factor of about 1 (forward currents), whereas positive voltages result in minor current variations (reverse currents) in the range of 10^{-13} A. In summary, Al contacts on H-terminated diamond give rise to perfect diode characteristics.

3.3 *Capacitance-voltage (CV) experiments*

Capacitance-voltage (*CV*) experiments on these contacts were carried out at $T = 300$ K using a Boonton 7200 capacitance meter in the reverse regime of the diodes. Typical *CV*-data are shown in Fig. 8 for contact sizes 50×50 μm^2, 100×100 μm^2 and 250×250 μm^2.[28] It is important to note that the capacitance is very small with values $C \leq 1$ pF in the regime –3 V

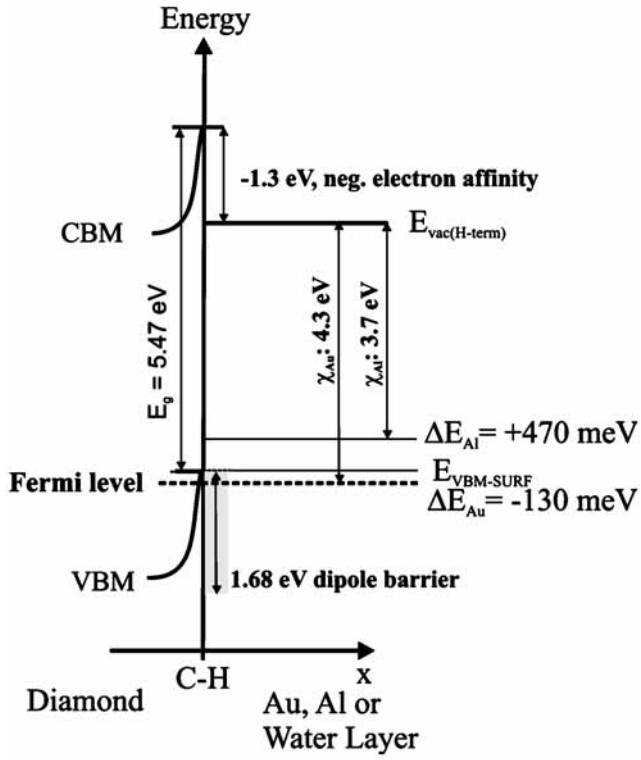

Fig. 5. Schematic energy band diagram of the interface of H-terminated diamond covered with Au or Al. The ΔE_{Al} and ΔE_{Au} refer to the valence band maximum at the surface, $E_{VBM\text{-}SURF}$.

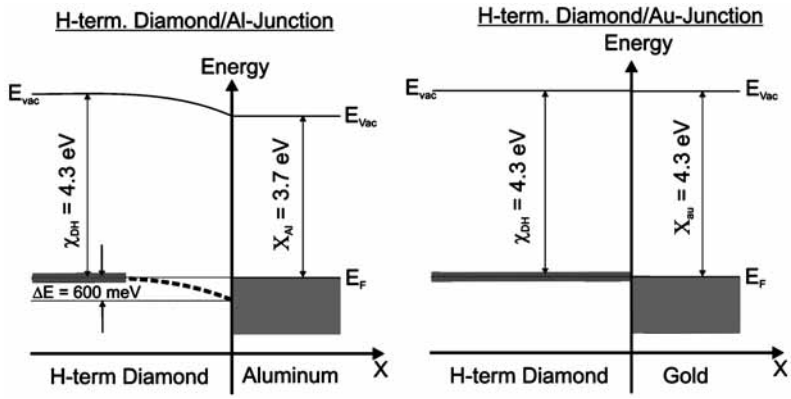

Fig. 6. Schematic surface energy diagrams of H-terminated diamond covered with an adsorbate layer which is in contact with aluminum and with gold. The data was calculated using contact potential difference experiments and assuming a negative electron affinity of –1.1 eV.

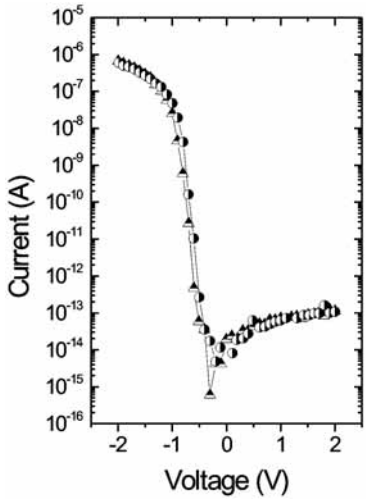

Fig. 7. Two *IV* characteristics measured on Al/H-terminated diamond Schottky junctions in air at T = 300 K with 250 μm × 250 μm contact size.

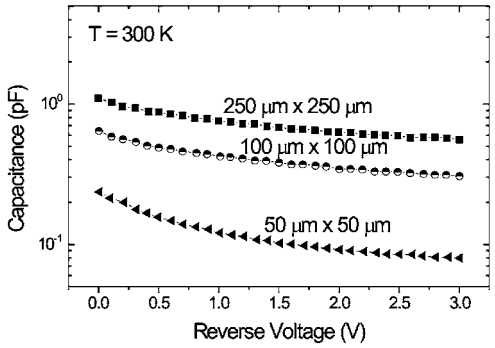

Fig. 8. Capacitance-voltage data detected on three contact configurations with Al areas 250×250 μm^2, 100×100 μm^2 and 50×50 μm^2.

$\leq V \leq 0$ V. If we assume a three-dimensional parallel-plate capacitor, the capacitance C can be calculated by

$$C = \varepsilon_o \varepsilon_r (A/d), \tag{1}$$

where ε_o is the dielectric constant, ε_r is the relative dielectric constant of diamond (ε_r = 5.7), A is the area of the Al contact, and d is the depletion layer width or the distance between the Al top contact and the doping layer. Considering an area of 250×250 μm^2 and a distance of 10 nm between the Al contact and a H-induced doping layer, the capacitance would be about 310 pF. We detect, however, much smaller values of typically ≤ 1 pF on all contacts realized.

In addition, the capacitance follows an approximately linear relationship with the length of the periphery of the Al contact, as shown in Fig. 9. We therefore conclude that no charge is below the Al contact, as expected for intrinsic diamond. The diode characteristic is governed by in-plane properties, where a p-type channel exists at the surface of hydrogen-terminated diamond. This channel does not exist below the Al. The p-type channel is connected with the metal if no energy barrier is present, as in the case of Au. In the case of work function differences, the energy gap generates in-plane Schottky properties that are comparable to 3D Schottky junctions. Such junction properties have been discussed in detail by Petrosyan *et al.*[29] and by Gelmont *et al.*[30]

4. Two-Dimensional Properties of a Perfect H-Terminated Diamond Surface

Figure 2 shows a schematic view of the electronic properties at the surface of H-terminated diamond, where valence-band electrons can tunnel into the empty electronic states of an adsorbate layer. The tunneling gives rise to band bending, which decreases in diamond with increasing distance to the surface. To calculate the width of the band bending, one has to take into account that depleted electronic states are valence band states where three bands have to be considered, namely the light hole (LH), the heavy hole (HH) and the split-off (SO) bands. The band structure of diamond is described by the Luttinger parameter and has been discussed in detail by Willatzen, Cardona and Christensen.[31] They derive the Luttinger parameter given by $\gamma_1 = 2.54$, $\gamma_2 = -0.1$, and $\gamma_3 = 0.63$.

To calculate the band bending in the vicinity of the surface of diamond we used a numeric approach that has been developed to solve the Schrödinger and Poisson equations simultaneously to calculate the energy levels in narrow GaAs/$Ga_{1-x}Al_xAs$ heterojunctions. Details can be found in ref. 32. In the case of band bending over a distance that is shorter than the

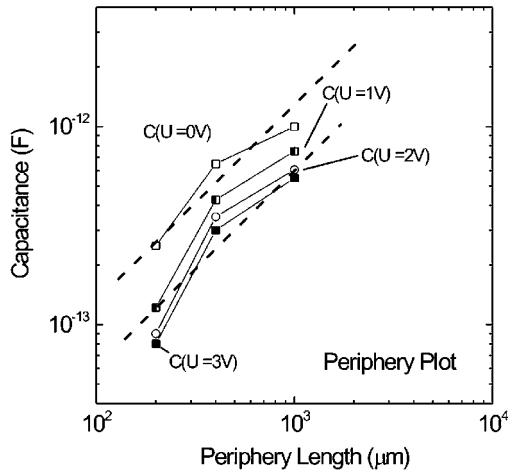

Fig. 9. Capacitance of the Al contacts with sizes 50×50 μm², 100×100 μm² and 250×250 μm² plotted for U = 0, 1, 2 and 3 V as a function of periphery length (dashed lines are a guide for the eye for linear dependence).

De Broglie wavelength of about 100 Å for holes (in diamond), the three-dimensional (3D) density-of-states (DOS) changes to a two-dimensional (2D) DOS, as shown schematically in Fig. 2(b). For this calculation the heterojunction effect is modeled using a graded interface in which the barrier height, as well as the effective mass, is assumed to change smoothly in a transition layer whose thickness is specified. Holes move in an effective potential given by

$$V(x) = e\phi(x) + V_h(x), \tag{2}$$

where $\phi(x)$ is the electrostatic potential and $V_h(x)$ is the effective potential energy associated with the heterojunction discontinuity, which we assume to be 1.68 eV.[33] The normalized envelope function $\zeta_i(x)$ for hole subband i is given by the Schrödinger equation of the BenDaniel-Duke form:

$$-\frac{\hbar^2}{2}\frac{d}{dx}\frac{1}{m_n(z)}\frac{d\zeta_i(x)}{dx} + V(x)\zeta_i(x) = E_i\zeta_i(x), \tag{3}$$

where $m_n(x)$ is the position-dependent effective mass (n stands for: HH, LH, SO) and E_i is the energy of the bottom of the i-th subband. The Poisson equation for the electrostatic potential takes the form

$$\frac{d}{dz}\varepsilon_o\varepsilon_r(x)\frac{d\phi(x)}{dx} = e\sum N_i\zeta_i^2(x) - \rho_I(x), \tag{4}$$

$$N_i = \frac{m_n kT}{\pi\hbar^2}\ln\left[1+\exp\left(\frac{E_i - E_F}{kT}\right)\right], \tag{5}$$

where $\varepsilon_r(x)$ is the position-dependent dielectric constant, which is assumed to be constant in diamond ($\varepsilon_r = 5.7$). For the adsorbate layer we varied ε_r between 1 and 5.7. The calculations show that ε_r does not affect the energy levels in the quantum well but does affect the width of the wave function of holes extending out of the diamond into the water layer. In the following we show results deduced for $\varepsilon_r = 5.7$. N_i is the number of holes per unit area in the subband i, E_F is the Fermi energy and m_n represents the mass of holes (HH, LH, SO). As a first order approximation we neglect impurities ($\rho_I(x) = 0$). Calculations have been performed for hole sheet densities in the range of 5×10^{12} cm^{-2} to 5×10^{13} cm^{-2}.

A typical result is shown in Fig. 10. At the interface to the H-terminated surface, three discrete energy levels for holes govern the electronic properties, namely, the first subbands of the LH-, HH- and SO-holes. For a hole sheet density of 5×10^{12} cm^{-2}, levels at 221 meV (HH), 228 meV (SO) and 231 meV (LH) below the VBM_{INT} are present. The Fermi energy is 237 meV below VBM_{INT}. Also shown are normalized hole wave-functions labelled LH, HH and SO. In thermodynamic equilibrium the chemical potential of the adsorbate layer and the Fermi level of diamond are in equilibrium. Our calculations reveal an energy gap between electrons in the adsorbate layer and holes in the quantum well. In the case of holes of 5×10^{12} cm^{-2}, they must overcome 6 meV or more to recombine with electrons. The wave-

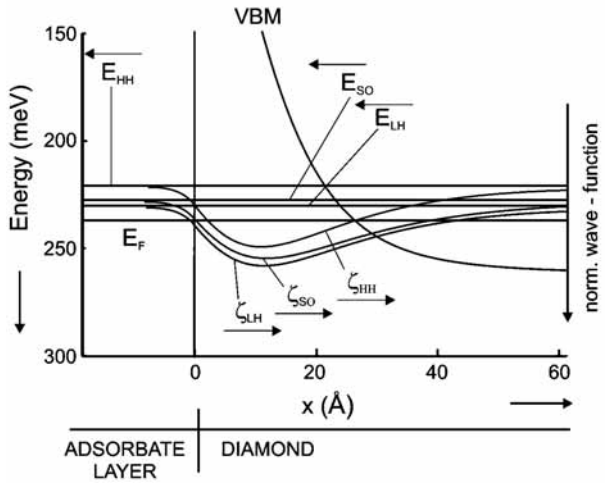

Fig. 10. Energy band diagrams at the interface of hydrogen-terminated diamond and an adsorbate layer calculated for hole sheet densities of 5×10^{12} cm^{-2}. The energies refer to the valence band maximum at the interface (VBM_{INT}). The figures show the calculated energy levels of the first subbands of the light hole (LH), heavy hole (HH) and split-off band (SO). Also drawn are the normalized wave functions ζ of holes (LH, SO, HH).

function of the holes extends about 5 Å into the adsorbate layer calculated for a dielectric constant ε_r of 5.7. For a hole sheet density of 5×10^{13} cm^{-2}, three discrete energy levels are calculated, 770 meV (HH), 786 meV (SO) and 791 meV (LH) below the VBM_{INT}. The first three sublevels are occupied by holes and recombination is prevented by a gap of 90 meV.

The 2D electronic DOS at a real surface is governed by 1) transfer doping properties (pH dependent), 2) surface smoothness, 3) hydrogen termination (surface defects), 4) defect passivation in diamond at the surface by hydrogen, and 5) ions in the Helmholtz layer of the adsorbate film. In addition, no conductive channel is present after thermal annealing (evaporation) of the adsorbate layer, which generates a perfectly insulting surface with a negative electron affinity.

5. Discussion of Capacitance-Voltage Data for Al

The capacitance-voltage data shown in Figs. 8 and 9 indicate that a peripheral depletion layer is present (see Fig. 9) between Al and H-terminated diamond that is covered with an adsorbate layer to generate transfer doping. This is schematically displayed in Fig. 6. Towards the Al contact, the accumulation layer is depleted as the work function of Al relative to H-terminated diamond is misaligned. This depletion region generates an in-plane capacitance which can be detected experimentally and which scales approximately with the length of the periphery (Fig. 9). The contacts were square, so some deviation is expected from a perfect fit, as corners cause some special effects in such experiments. In the future, such experiments should be performed using contacts with rotational symmetry. The data indicate that in-plane Schottky-junction (2D) properties of Al on H-terminated diamond dominate the electronic properties.

General features of a junction between a two-dimensional electron gas and a metal contact with Schottky properties have been discussed by S. G. Petrosyan and A. Y. Shik (1989)[29] and by B. Gelmont and M. Shur (1992).[30] Following their arguments the capacitance of a metal in contact with a 2D gas is well described by

$$C = \frac{\varepsilon_o \varepsilon_r L}{\pi} \ln\left\{\frac{\left(d_{Al}^2 + x_{dep}^2\right)^{0.5} + d_{Al}}{\left(d_{Al}^2 + x_{dep}^2\right)^{0.5} - d_{Al}}\right\}, \tag{6}$$

where L is the length of the metal periphery, d_{Al} is the thickness of Al and x_{dep} is the width of the space charge region. Taking into account the Al thickness of 600 nm, $\varepsilon_r = 5.7$, and the detected variation of the capacitance, the variation in the depletion width in our experiments is in the range of 10 to 300 nm (see Fig. 11). The shortness of the depletion layer is a result of the high hole sheet carrier density, which is in the range 10^{12} to 10^{14} cm^{-2}. Petrosyan and Shik[29] calculated an inversely proportional relationship between the width of the depletion layer and the sheet carrier density, which was given by:

$$x_{dep} \propto \frac{\varepsilon_o \varepsilon_r}{2\pi e} \frac{V}{p_{sh}}, \tag{7}$$

where V is the applied voltage, e is the elementary charge, and p_{sh} is the sheet hole density. It is interesting to note that such an in-plane (2D) junction also follows the exponential law given by ref. 29:

$$j \approx j_{rev}\left[\exp\left(\frac{eU}{kT}\right) - 1\right], \tag{8}$$

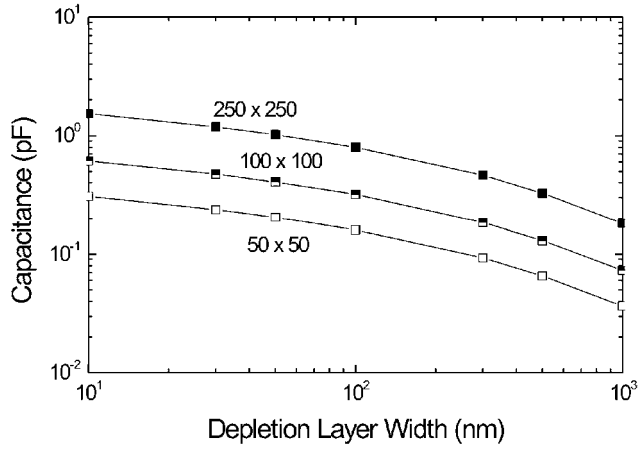

Fig. 11. Calculated capacitance variations as a function of width of the depletion layer. Experimentally the capacitance is in the range 0.06 pF to 1 pF, which shows that the depletion layer width varies between 10 and 300 nm.

where j_{rev} is the contact specific reverse current (for details see ref. 29). To summarized these results briefly: The detected absolute values of the capacitance are orders of magnitude too small to be discussed using a parallel plate model. The most reasonable model is an in-plane Schottky model. Unfortunately, such junctions show comparable characteristics to three dimensional (conventional) Schottky junctions and are therefore not distinguishable if only *IV* experiments are applied. Only a combination of *CV* and *IV* reveal the true properties.

6. Carrier Propagation and Scattering

To characterize the propagation of holes in the accumulation layer, we have performed temperature-dependent Hall-effect experiments on a variety of H-terminated diamond films. In the following we focus on the results deduced for one H-terminated diamond sample which shows high-quality bulk properties and which has a very smooth surface (atomically flat). Hydrogen termination has been carried out with parameters summarized in Table 1 (AIST). To vary the electronic properties, the sample has been treated as follows: a) exposed for 3 days to humid air, inserted into the Hall setup (base pressure 1 Torr), heated to 400 K and kept at 400 K for 60 min before the Hall experiment started. b) After the first experimental cycle (a), Hall experiments were carried out again in which the sample was first heated to 400 K and held at 400 K for 30 min before the Hall experiments started. c) The sample was cleaned mechanically to remove a graphitic layer that had been detected by contact mode AFM, electron microscopy and wetting angle experiments, and then measured as described for case (a).

The results are summarized in Figs. 12 and 13, where hole sheet densities and mobilities are plotted as a function of temperature. Data, plotted by full squares, are detected in the first

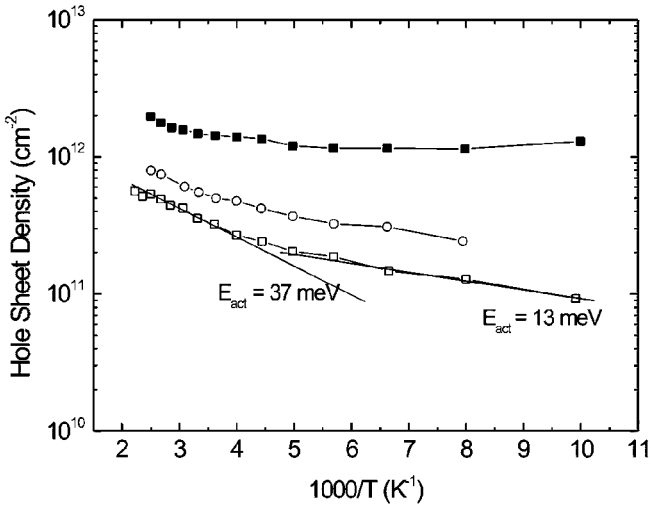

Fig. 12. Hole sheet-carrier densities measured for two different conditions on the same sample. The straight lines are fits to the data to calculate the activation energies, which are 37 and 13 meV.

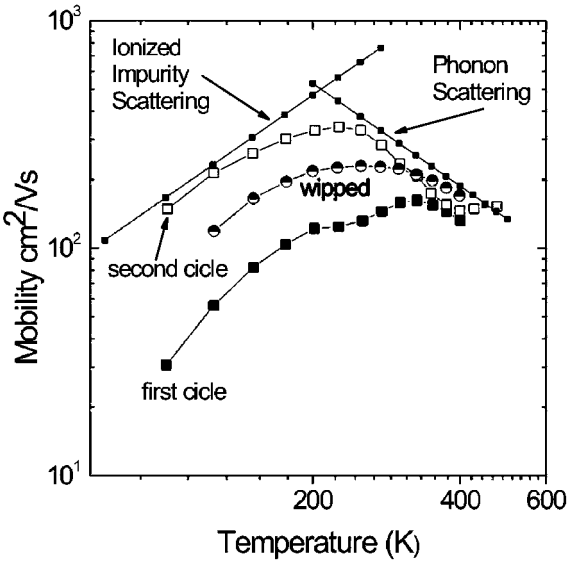

Fig. 13. Hole mobilities measured for two different conditions on the same sample. The data were detected on the same layer as shown in Fig. 12. Straight lines indicate the rise expected by ionized impurity scattering or the decrease due to phonon scattering.

Hall measurement cycle a) after exposing the surface for an extended period of time to air (more than 3 days) without mechanical cleaning. In this case the hole sheet density is weakly temperature dependent, showing a decrease from 2×10^{12} cm^{-2} at 400 K to 1.2×10^{12} at 100 K. The second Hall experiment (case (b)) was applied after cycle (a) without breaking the 1 Torr vacuum, but after annealing the layer for about 30 min at 400 K. This date is shown as open squares. The thermal annealing at 400 K gives rise to a decrease in the hole sheet density, which varies between 6×10^{11} cm^{-2} at 400 K and 10^{11} cm^{-2} at 100 K. The density is slightly activated at about 13 meV at low temperatures, rising to 37 meV at higher temperatures (see solid lines in Fig. 12). Exposing the film to air for an extended period of time recovers the initial properties (detected in cycle (a)) or heating the sample for several hours at 550 K gives rise to insulating properties which can be converted to conductive properties by exposing the sample to air. The data support the results of other groups who demonstrated that the application of annealing treatments gives rise to conductivity variations, as described previously.

Due to the hydrogenation process, we detected a carbon layer on all samples by AFM and electron microscopy. This layer can be removed by mechanical cleaning. After such a treatment we performed Hall-effect experiments again as in cycle (a) and found that the hole sheet density was affected by surface cleaning. The hole-sheet density and the mobility are somewhere between the results of the first (cycle (a)) and second (cycle (b)) Hall-effect measurements. Obviously, the interaction of the clean hydrogen terminated diamond surface with the adsorbate layer changes. Further experiments are, however, needed to elucidate the details of this process.

These results support the transfer-doping model. In this model, the activation energy of holes is not due to thermal activation from acceptor states (classical doping) but the energy represents the trapping of holes in localized electronic states which are present at the surface of H-terminated diamond. The origin of these traps may be attributed to surface roughness, imperfect H termination and ion-induced potential modulation where ions in the Helmholtz layer of the adsorbate give rise to Coulomb scattering in the p-type channel.

In the following we discuss the variation in the hole mobility as function of temperature, which is shown in detail in Fig. 12. Generally, an increase of mobility is detected with decreasing hole sheet density. This is in agreement with data summarized in Fig. 1. For the first time, however, a "semiconductor" type of temperature dependence was detected with a maximum mobility at around 230 K of 340 cm^2/Vs. Toward lower or higher temperatures the mobility decreased. Also shown are the schematic variations due to ionized impurity scattering following a $\mu \approx T^{-1.5}$ dependence toward lower temperatures and phonon scattering, which gives rise to a $\mu \approx T^{+1.5}$ dependence, toward higher temperatures.

In the case of transfer doping, the density of ions in the Helmholtz layer (ionized impurity centers) is known, as it is exactly the number of holes in the accumulation layer. The negatively charged ions are distributed in the adsorbate film where they accumulate in the Helmholtz layer, as shown schematically in Fig. 14. To discuss the scattering problem in terms of absolute numbers, we take the density of holes detected at the highest temperatures, where all holes are mobile, and assume that this is the density of "ionized impurities." Ionized impurity scattering dominates carrier propagation at low temperatures, so we take the mobilities detected at 125 and 150 K into account for this discussion. According to a well-established formula, ionized impurity scattering is inversely proportional to the density of ionized impurities (N_I):

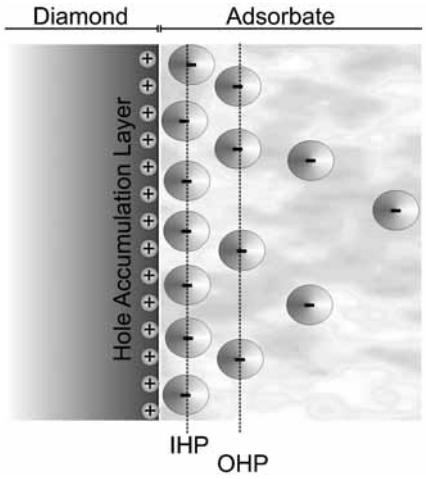

Fig. 14. Schematic description of the interface of a H-terminated diamond with a hole accumulation surface layer and the Helmholtz layer of the adsorbate film which covers the diamond (IHP: inner Helmholtz plane, OHP: outer Helmholtz plane). The + sign represents holes propagating at the surface and the – sign indicates negatively charged ions in the liquid, which accumulated in the Helmholtz layer.

$$\mu \approx \frac{1}{N_I}. \tag{9}$$

Figure 15 shows the result, where the mobilities measured at T = 125 K and 150 K are plotted as a function of sheet hole density (= ionized impurity density). This is in perfect agreement with the prediction (dashed line). We conclude, therefore, that the mobility in the hole accumulation layer of H-terminated diamond is limited at low temperature by ionized impurity scattering. The impurities are in the Helmholtz layer of the adsorbate film, very close to the hole accumulation layer in diamond. The model has limits as the density of ions is not distributed homogenously in the bulk, but accumulated in a layer adjacent to the hole channel. As this layer, however, is very close to holes, the scattering may be comparable to a three dimensional case. We applied other known scattering mechanisms, which are summarized in the article by Ando, Fowler and Stern;[34] however, only the scattering model discussed herein gives reasonable agreement with our experimental data. Scattering by adsorbate ions indicates limitations of the electronic applications of such heterojunctions. The hole channel and the ionized impurities are too close to achieve ultrahigh mobilities as in the case of GaAs/AlGaAs high-electron-mobility transistors.

To summarize: We discussed the variation in mobilities using scattering laws derived for bulk material (3D case). This has been done by intent, as the mobilities are still so low that a 2D discussion makes no sense (for a review, see ref. 34). This may be a result of Coulomb disorder, which arises from the ions in the Helmholtz layer of the adsorbate film. These potential variations at the surface may be too strong for a truly 2D electronic system in the characterized temperature regime. To achieve further optimization, a spacer may be required, such as C60 or other forms of carbon.[35]

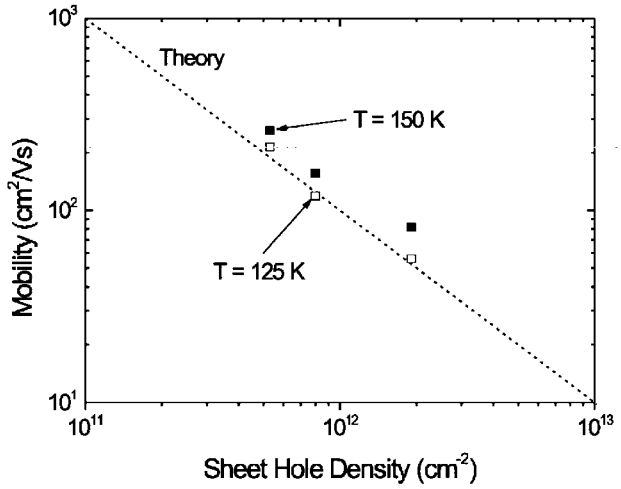

Fig. 15. Experimentally detected decrease in hole mobilities with increasing hole sheet density. The dashed line represents the prediction following ionized impurity scattering.

7. Summary

Hydrogen-terminated diamond covered by an adsorbate layer shows electronic properties which can be discussed using the transfer doping model. The electronic properties are governed by the alignment of the Fermi level with the chemical potential of the adsorbate layer. Depending on thermal treatments, the ion density in the adsorbate layer changes, which gives rise to variations in the carrier sheet densities and the hole mobilities. Metals evaporated on top of H-terminated diamond such as Au (ohmic contact) and Al (Schottky contact) generate contact properties that are well described with an "in-plane" contact model, in which the work function of the metal can be used to discuss the contact properties with respect to the electron affinity of H-terminated diamond.

Theoretical calculations of the ideal surface electronic properties of H-terminated diamond in contact with an adsorbate layer result in 2D properties with discrete energy levels. The calculated energies are in reasonable agreement with contact potential difference experiments applied to the samples. However, truly 2D properties can only be expected if the surface is atomically smooth, the hydrogen termination is perfect, and the ions in the Helmholtz layer of the adsorbate film do not interact too strongly by Coulomb scattering. It has been shown[36] that atomically smooth surfaces can be grown by CVD plasma techniques. In addition, there is evidence that hydrogen termination of diamond gives rise to an unpinned surface Fermi level, which indicates that the surface defect density is very small.[37] For the technological establishment of an electronic device based on such a transfer doping effect, the use and optimization of a spacing layer would be favorable. Increasing the distance of ions in the Helmholtz layer of the adsorbate film with respect to the hole accumulation layer would minimize the scattering of holes and most likely reduce potential variations that give rise to carrier trapping. We assume that in our case the distance is in the Angstrom regime. As C60 has been demonstrated to generate transfer doping if deposited in more than 8 atomic layers,[35] this is a promising candidate for a spacer.

Acknowledgements

The author thanks Dr. B. Rezek for contact potential difference experiments, Dr. H. A. Garrido for *CV* and *IV* experiments, and Prof. A. Zrenner for the theoretical calculations of the surface electronic properties.

References

1) F. Maier, J. Ristein and L. Ley: Phys. Rev. B **64** (2001) 165411.
2) M. I. Landstrass and K. V. Ravi: Appl. Phys. Lett. **55** (1989) 975.
3) T. Maki, S. Shikama, M. Komori, Y. Sakaguchi, K. Sakuta and T. Kobayashi: Jpn. J. Appl. Phys. **31** (1992) 1446.
4) K. Hayashi, S. Yamanaka, H. Okushi and K. Kajimura: Appl. Phys. Lett. **68** (1996) 376.
5) H. J. Looi, R. B. Jackman and J. S. Foord: Appl. Phys. Lett. **72** (1998) 353.
6) R. I. S. Gi, K. Tashiro, S. Tanaka, T. Fujisawa, H. Kimura, T. Kurosu and M. Iida: Jpn. J. Appl. Phys. **38** (1999) 3492.
7) O. A. Williams and R. B. Jackman: Diamond Relat. Mater. **13** (2004) 325.

8) O. A. Williams and R. B. Jackman: Semicond. Sci. Technol. **18** (2003) S34.
9) O. A. Williams, M. D. Whitfield, R. B. Jackman, J. S. Foord, J. E. Butler and C. E. Nebel: Diamond Relat. Mater. **10** (2001) 423.
10) O. A. Williams and R. A. Jackman: Diamond Relat. Mater. **13** (2004) 166.
11) H. J. Looi, L. Y. S. Pang, A. B. Molloy, F. Jones, J. S. Foord and R. B. Jackman: Diamond Relat. Mater. **7** (1998) 550.
12) N. Jiang and T. Ho: J. Appl. Phys. **85** (1999) 8267.
13) K. Hayashi, S. Yamanaka, H. Watanabe, T. Sekigachi, H. Okushi and K. Kajimura: J.Appl. Phys. **81** (1997) 744.
14) C. E. Nebel: unpublished data.
15) H. Watanabe, K. Hayashi, D. Takeuchi, S. Yamanaka, H. Okushi and K. Kajimura: Appl. Phys. Lett. **73** (1998) 981.
16) B. Rezek, C. Sauerer, C. E. Nebel, M. Stutzmann, J. Ristein, L. Ley, E. Snidero and P. Bergonzo: Appl. Phys. Lett. **82** (2003) 2266.
17) H. Kawarada: Surf. Sci. Rep. **26** (1996) 207.
18) R. I. S. Gi, T. Mizumasa, Y. Akiba, H. Hirose, T. Kurosu and M. Iida: Jpn. J. Appl. Phys. **34** (1995) 5550.
19) J. Shirafuji and T. Sugino: Diamond Relat. Mater. **5** (1996) 706.
20) F. Maier, M. Riedel, B. Mantel, J. Ristein and L. Ley: Phys. Rev. Lett. **85** (2000) 3472.
21) H. Kiyota, E. Matsushima, K. Sato, H. Okushi, T. Ando, M. Kamo, Y. Sato and M. Iida: Appl. Phys. Lett. **67** (1995) 3596.
22) S. Albin and L. Watkins: Appl. Phys. Lett. **56** (1990) 1454.
23) C. E. Nebel, C. Sauerer, F. Ertl, M. Stutzmann, C. F. O. Graeff, P. Bergonzo, O. A. Williams and R. Jackman: Appl. Phys. Lett. **79** (2001) 4541.
24) C. E. Nebel, F. Ertl, C. Sauerer, M. Stutzmann, P. Bergonzo, H. Okushi, O. A. Williams and R. Jackman: Diamond Relat. Mater. **11** (2002) 351.
25) D. Takeuchi, H. Kato, G. S. Ri, T. Yamada, P. R. Vinod, D. Hwang, C. E. Nebel, H. Okushi and S. Yamasaki: Appl. Phys. Lett. **86** (2005) 152103.
26) J. C. Angus, Y. V. Pleskov and S. C. Eaton: in *"Thin Film Diamond II," Semiconductors and Semimetals*, Vol. 77, Eds. C. E. Nebel and J. Ristein (Elsevier, Amsterdam, 2004) p. 97.
27) W. Mönch: in *"Semiconductor Surfaces and Interfaces," Surface Sciences, Springer*, 1995.
28) J. A. Garrido, C. E. Nebel, M. Stutzmann, E. Snidero and P. Bergonzo: Appl. Phys. Lett. **81** (2002) 637.
29) S. G. Petrosyan and A. Y. Shik: Sov. Phys. Semicond. **23** (1989) 696.
30) B. Gelmont and M. Shur: IEEE Trans. on Electron Devices **39** (1992) 1216.
31) M. Willatzen, M. Cardona and N. E. Christensen: Phys. Rev. B **50** (1994) 18054.
32) F. Stern and S. DasSarma: Phys. Rev. B **30** (1984) 840.
33) J. Ristein, F. Maier, M. Riedel, J. B. Cui and L. Ley: Phys. Status Solidi A **181** (2000) 65.
34) T. Ando, A. B. Fowler and F. Stern: Rev. Mod. Phys. **54** (1982) No. 2.
35) P. Strobel, M. Riedel, J. Ristein and L. Ley: Nature **430** (2004) 439.
36) H. Okushi, H. Watanabe, S. Ri, S. Yamanaka and D. Takeuchi: J. Cryst. Growth **237** (2002) 1269.
37) D. Shin and C. E. Nebel: private communication.